EJN European Journal of Neuroscience

FENS Federation of European Neuroscience Societies

European Journal of Neuroscience, Vol. 44, pp. 2357–2368, 2016 doi:10.1111/ejn.13334

COGNITIVE NEUROSCIENCE

Timing matters: open-loop stimulation does not improve overnight consolidation of word pairs in humans

Arne Weigenand,[1,2] Matthias Mölle,[3,4] Friederike Werner,[5] Thomas Martinetz[1,2] and Lisa Marshall[2,5]
[1]Institute for Neuro- and Bioinformatics, University of Lübeck, Ratzeburger Allee 160, 23562 Lübeck, Germany
[2]Graduate School for Computing in Medicine and Life Science, University of Lübeck, Lübeck, Germany
[3]Center for Brain, Behavior and Metabolism, University of Lübeck, Lübeck, Germany
[4]Institute for Medical Psychology and Behavioral Neurobiology, University of Tübingen, Tübingen, Germany
[5]Institute of Experimental and Clinical Pharmacology and Toxicology, University of Lübeck, Ratzeburger Allee 160, 23562 Lübeck, Germany

Keywords: memory, sleep, slow oscillations, spindles, thalamocortical system

Edited by Sophie Molholm
Received 8 March 2016, revised 13 June 2016, accepted 6 July 2016

Abstract

The application of auditory clicks during non-rapid eye movement (NREM) sleep phase-locked to the up state of the slow oscillation (closed-loop stimulation) has previously been shown to enhance the consolidation of declarative memories. We designed and applied sequences of three clicks during deep NREM sleep to achieve a quasi-phase-dependent open-loop stimulation. This stimulation was successful in eliciting slow oscillation power in the stimulation period. Although fast and slow spindle power were markedly decreased during the stimulation period, memory consolidation did not differ from control. During putative up states fast spindle power remained, however, at control levels. We conclude that concurrence of slow oscillations and fast spindles suffices to maintain memory consolidation at control levels despite an overall decreased spindle activity.

Introduction

Spindle oscillations and large amplitude slow oscillations are the hallmarks of NREM sleep in the EEG. Together with hippocampal ripples they play a key role in the sleep-dependent consolidation of declarative memories and synaptic plasticity (Rosanova & Ulrich, 2005; Chauvette *et al.*, 2012; Rasch & Born, 2013). Underlying slow oscillations (SO) are widespread transient alternations of cortical networks between active and silent phases at around 1 Hz (Contreras & Steriade, 1995; Weigenand *et al.*, 2014). Spindles are thought to arise from interactions between neurons of the thalamic reticular nucleus and thalamocortical neurons of other thalamic nuclei (Destexhe & Sejnowski, 2003). At least two major types of spindles can be distinguished, which differ in frequency, topography and possibly function: slow spindles (9–12 Hz), that are found at frontal cortical sites, and fast spindles (12–15 Hz) with centro-parietal prevalence (Kandel & Buzsaki, 1997; Anderer *et al.*, 2001; Mölle *et al.*, 2011). The full expression of spindle and slow oscillation rhythms depends on the interplay of the thalamus and neocortex (Bonjean *et al.*, 2011; David *et al.*, 2013; Sheroziya & Timofeev, 2014). Spindles and ripples can occur independently of SOs, but appear at a higher rate during the depolarized up states of SOs (Mölle *et al.*, 2006; Clemens *et al.*, 2007; Peyrache *et al.*, 2011).

This temporal grouping has been suggested to be critical for hippocampus-dependent memory consolidation as learning-dependent increases in spindle activity are restricted to the SO up state (Mölle & Born, 2011; Cox *et al.*, 2012; Niknazar *et al.*, 2015). In order to shed light onto the specific contributions of SOs, ripples and spindles to memory consolidation, one may selectively suppress or enhance them by experimental intervention (Marshall *et al.*, 2006; Girardeau *et al.*, 2009; Ego-Stengel & Wilson, 2010; Ngo *et al.*, 2013).

A recent study in humans showed that two-click auditory stimulation in phase with positive half-waves of endogenous SOs ('closed-loop stimulation') is capable of improving performance in a verbal paired-associate learning task (Ngo *et al.*, 2013). This result has been reproduced with more than two clicks, also relying on phase-dependent stimulation (Ngo *et al.*, 2015). Although spindles and SOs seem to be involved, the specific aspect of the closed-loop stimulation paradigm responsible for the improvement remains unclear.

We tested whether a similar effect on learning performance can be achieved with a rhythmic click sequence. The rhythmic sequence also achieves in-phase stimulation, but starts at a random phase of the SO. The stimulation paradigm, termed open-loop stimulation in

Correspondence: Arne Weigenand, [1]Institute for Neuro- and Bioinformatics, University of Lübeck, as above.
E-mail: weigenand@inb.uni-luebeck.de
and
Lisa Marshall, [5]Institute of Experimental and Clinical Pharmacology and Toxicology, University of Lübeck, as above.
E-mail: lisa.marshall@pharma.uni-luebeck.de

the following, is based on the observation that a single click has a high probability of evoking a single SO or a K-complex (KC) given some time has passed since the last click (Bastien & Campbell, 1994). We used the first click in a sequence to evoke a SO, thereby resetting the ongoing activity to a known phase. Using a defined interval, a subsequent click can then be delivered during the up state of the evoked SO.

Materials and methods

Participants

Twenty-six healthy right-handed volunteers participated in this study, of which 21 (11 male, mean age 22.2 years, range 18–28 years) were used for the analysis. Five participants left the study before completion. The experimental protocol was approved by the ethics committee of the University of Lübeck and all volunteers gave their written consent prior to participation.

The subjects were native German speakers, non-smokers and had no history of neurological, psychiatric or endocrine disorders. Furthermore, all participants were free from medication except the females, who were all taking hormonal contraceptives. Participants slept 7–9 hours per night, did not normally take daytime naps and followed a regular sleep schedule as assessed by interview and questionnaire. They reported no major disruptions of the sleep–wake cycle during the 4 weeks before experimentation. Subjects were instructed to abstain from alcohol and caffeine and to get up at 6:00 h on the day of the experiment.

Experimental design and procedures

This study followed a single-blind, counterbalanced crossover design. Each subject participated in one adaptation night, and two experimental nights of either a 'Stimulation' or a 'Sham' session. Experimental nights were separated by at least 1 week to avoid carry-over effects. Experimental sessions started at 20:30 h with the application of EEG electrodes. Each session consisted of a learning phase followed by an immediate recall phase with feedback and subsequent sleep from 23:00 to 6:00 h., with either auditory or sham stimulation. A second recall in the morning (6:30 h) served to assess overnight retention. The experimental design is summarized in Fig. 1A. (Note that feedback at immediate test does not allow for assessment of a real baseline.)

EEG recordings and polysomnography

EEG was recorded throughout the whole night using a BrainAmp DC amplifier (Brain Products) from 21 channels according to the international 10–20 system (Fp1, Fpz, Fp2, F7, F3, Fz, F4, F8, T3, C3, Cz, C4, T4, T5, P3, Pz, P4, T6, O1, Oz, O2), referenced to linked mastoid electrodes. Ag-AgCl electrodes were used and impedances were below 5 kΩ. Signals were low-pass filtered (f_{cutoff} = 120 Hz), sampled at 500 Hz and stored for later offline analysis on a PC together with the stimulation triggers. For all subsequent analysis, data were down-sampled to 100 Hz. Vertical and horizontal eye movements (EOG) as well as electromyogram from the chin (EMG) were obtained for standard polysomnography and artifact detection. For the adaptation night, a reduced set of scalp electrodes was used (Fp1, Fpz, Fp2, F3, Fz, F4, C3, Cz, C4, P3, Pz, P4).

Each night was scored visually for succeeding 30-s epochs according to AASM criteria (Iber *et al.*, 2007) by an experienced sleep scorer blind to the condition.

Total sleep time (TST), time spent in different sleep stages (wake; sleep stages N1, N2, N3, REM) and the number of movement arousals were determined for the whole night and separately for the stimulation period and the remaining sleep time. Sleep onset, i.e. the first occurrence of sleep stage N2, was defined with reference to lights off.

Auditory stimulation

The stimulation protocol is outlined in Fig. 1B. In the stimulation condition, groups of three click sounds were delivered via in-ear headphones (Philips SHE 8500) during slow-wave sleep (sleep stage N3). A single click consisted of 50 ms of pink noise with a 5-ms rise and fall time. The timing of the second and third click relative to the first click was chosen to maximize their probability of coinciding with evoked SO up states, given that the preceding click triggers a SO.

Specifically, the delay between first and second click was chosen individually as the mean delay time between the first click and the maximum peak of the subject's succeeding large positive deflection at electrode Fz. This deflection reflects the presumed depolarizing up state of the evoked K-complex. The delay was assessed in the adaptation night using 60 clicks with inter-stimulus intervals of 5–9 s (uniformly distributed). The component is known as P900 in the evoked potential literature, since the positive peak occurs ca 900 ms after the stimulus (Bastien *et al.*, 2002).

The second and third clicks were 1.075 s apart, which was adopted from Ngo *et al.* (2013) and corresponded to the average duration of a SO. Click sequences were separated by 5–9 s (uniform scatter). In the sham condition, subjects wore in-ear headphones, but no clicks were generated.

The stimulation period always began after 5 min of stable N3, which was assessed online by the experimenter and continued for 210 min. When arousals or changes in sleep stage were detected, stimulation was paused. It was resumed when stable N3 was detected again. Signals were generated using a CED POWER1401 MKII programmed via SPIKE2 version 7.11 (Cambridge Electronic Design Limited, Cambridge, UK). Trigger markers of each tone were recorded in the stimulation condition. Trigger markers of the sham condition were generated offline and matched the markers of the stimulation condition in number, distribution of inter-stimulus intervals, number of stimulation epochs and start and end time of the stimulation period.

Paired-associate learning task

The word-pair memory task was adopted from a previous study (Ngo *et al.*, 2013). In brief, subjects had to memorize 120 German word pairs, which were presented sequentially on a monitor using E-PRIME 2.0 (Psychology Software Tools). Each item was displayed for 4 s with an inter-stimulus interval of 1 s between items. Two different word lists were used for the two experimental sessions and the order of word lists was balanced across subjects and conditions. Furthermore, the lists were matched in difficulty in order to reduce baseline variance. During the immediate recall phase, the subject had to respond by naming the second word upon presentation of the first word of a pair and had unlimited time to recall the appropriate word. The correct answer was revealed on the screen immediately after the response. At testing in the morning after sleep, cued recall was tested in the same manner as after learning, except that no feedback was given after the subject's response. Participants were explicitly advised to visualize word pairs as learning strategy and to

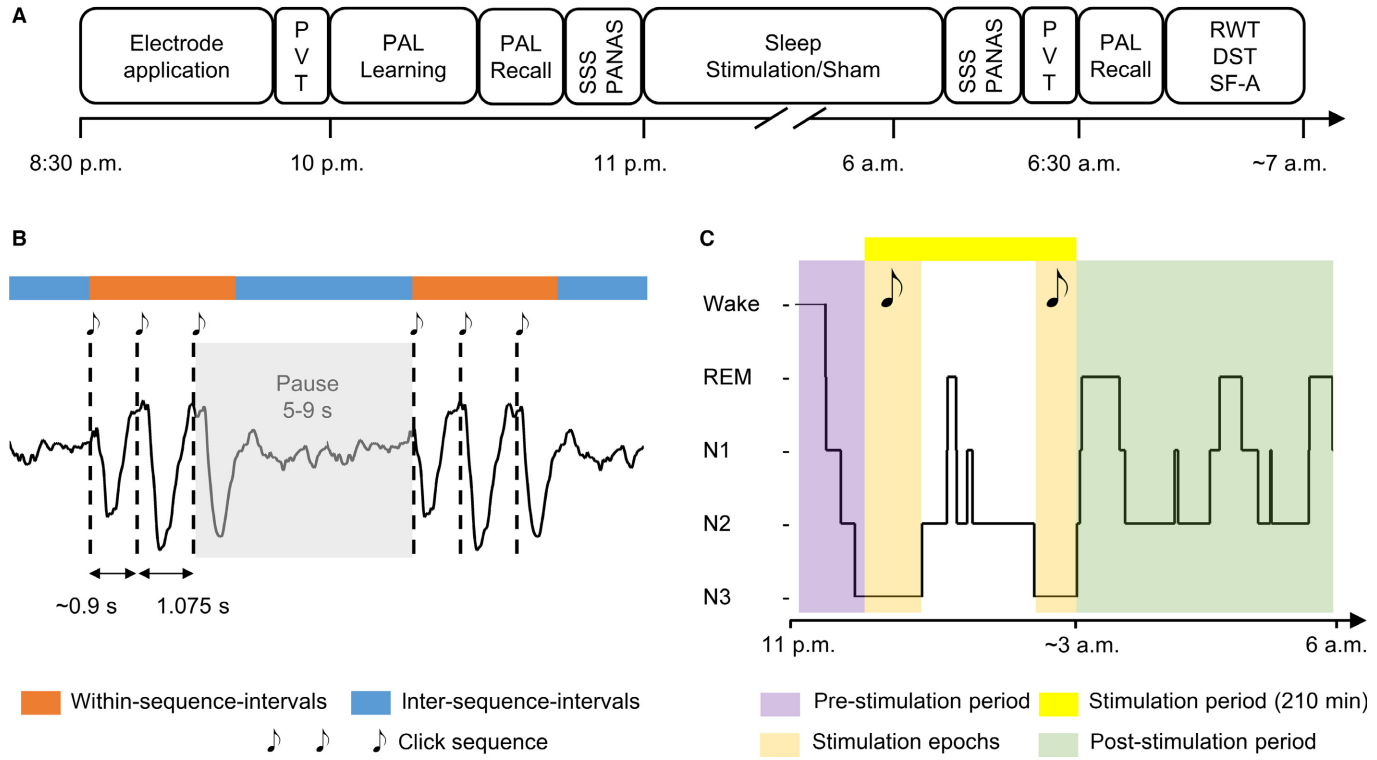

FIG. 1. Stimulation protocol. (A) Outline of experimental nights. PVT, psychomotor vigilance test; PAL, paired-associate learning; SSS, Standford Sleepiness Scale; RWT, Regensburg Word Fluency Test; DST, Digit Span Test; SF-A, Sleep Questionnaire A; PANAS, Positive and Negative Affect Schedule. (B) Sequences of three clicks were applied during N3. After a sequence of three clicks, there was a 5- to 9-s pause ('inter-sequence interval') between the last click and the first click of the following sequence. The first and last clicks of a sequence define the 'within-sequence interval'. The interval between the first and second clicks within a sequence was set to the average SO period of the respective subject, which was determined during the adaptation night from single-click evoked potentials at lead Fz. The interval between the second and third clicks was fixed to 1.075 s. The first click had a high probability to evoke a SO and, hence, was applied to induce a phase reset. The second and third clicks were then more likely to occur in phase with a SO up state. Essentially, the protocol is a phase-independent modification of the closed-loop auditory stimulation (Ngo *et al.*, 2013). (C) A hypnogram indicating the pre-stimulation period, stimulation period, stimulation epochs and post-stimulation period. Stimulation started after 5 min of stable N3 and only took place during N3 epochs of the 210 min stimulation period. Baseline effects were controlled for in the N2 epochs of the pre-stimulation period. NREM sleep epochs of the post-stimulation period were analyzed for after-effects.

guess instead of giving no answer. Only exact responses were considered correct.

Several control tests were performed to assess non-specific contributions of the stimulation to memory performance. Before and after sleep, the subjects' mood and tiredness were assessed with the Positive and Negative Affect Schedule (PANAS) and the Stanford Sleepiness Scale (SSS) (Hoddes *et al.*, 1973; Watson *et al.*, 1988). Sleep quality was assessed by means of questionnaire SF-A (Görtelmeyer, 1981). Additionally, a Digit Span Test (DST) and the Regensburg Word Fluency Test (RWT) were administered in the morning to control for general abilities to retrieve information from long-term memory and for working memory performance (Tewes, 1991; Aschenbrenner *et al.*, 2000). All subjects underwent a psychomotor vigilance test (PVT) to control for general alertness and vigilance. In this task, a counter appears at the center of a computer screen every 2–10 s for about 5 min and participants have to respond as quickly as possible by pressing a button. The behavioral data is summarized in Table S1.

Artifact detection

In a first step, epochs with artifacts were marked manually during scoring. Automatic resetting of DC offsets, sudden signal jumps, increased muscle tone (EMG signal) and drifts induced by sweating were regarded as artifacts. In a second step, an automatic algorithm classified epochs as artifactual if the difference between consecutive samples was > 100 μV or the SD of the epoch exceeded 150 μV. Epochs with artifacts were removed from the analysis. In the rare case where a single electrode detached or persistently exhibited artifacts, it was replaced by a combination of the remaining intact electrodes determined by linear regression.

Event-related potentials

Data were analyzed using MATLAB R2013a (The MathWorks, Inc., Natick, MA, USA). Event-related potentials of the EEG signal were obtained from the down-sampled raw data of which a linear trend was removed ±6 s around the first click of each sequence. This eliminated the influence of strong dc drifts without distorting the waveform. The number of windows used for averaging in the stimulation and sham conditions was on average 295 ± 119 and 287 ± 105 respectively.

Offline detection of SOs and K-complexes

The offline detection of SO/K-complex events is based on Mölle *et al.* (2002). A low-pass filter (Chebyshev type II, f_{stop} = 4.5 Hz, f_{pass} = 3.5 Hz, A_{stop} = 60 dB) and a high-pass filter (Butterworth, f_{stop} = 0.1 Hz, f_{pass} = 0.5 Hz, A_{stop} = 20 dB) were applied to the raw signal of the individual channel of interest. Then, all zero-

crossings were determined and negative and positive half-waves extracted. Segments having a negative half-wave with a width between 150 and 800 ms and exceeding a peak negativity of −65 μV were regarded as SOs and the negative half-wave peaks were used for the identification of the SO events. The validity of detected events was verified visually. Filters were applied in forward and reverse direction to eliminate phase distortion. SOs were considered to be evoked if they occurred within 200–900 ms following a click.

Event histogram

In order to examine whether our open-loop stimulation actually evoked SO events, delays between the first clicks of presented click sequences and offline detected SO events (all endogenous + evoked), using a bin size of 100 ms were assessed. The resulting histogram was then normalized using the total number of click sequences, yielding the corresponding probability, *P*. The analysis was limited to the interval [−2, 5] s around first click (at $t = 0$ s).

Spectral analysis

Power spectra were computed for all artifact-free 30 s epochs with Matlab's pwelch method using a Hanning window of 6 s length, 50% segment overlap and zero-padding to a total length of 20 s. The spectra of the epochs of interest, i.e. the N2 epochs of the pre-stimulation period, the stimulation epochs during NREM sleep of the stimulation period and the NREM sleep epochs of the post-stimulation period, were then averaged and subsequently normalized. The mean of the power of all channels between 0.3 and 30 Hz, both conditions and all NREM sleep epochs of the subject was used for normalization. This procedure maintains the within-subject variance, but reduces between-subject variance by levelling the large baseline differences between subjects common to spectral data. It has the additional benefit of improving Gaussianity of the data. Frequencies below 0.3 Hz were discarded for normalization, because they mainly comprise strongly varying DC and drift components. Finally, normalized spectral data were split into the following frequency bands: SO, 0.5–1 Hz, Delta, 1–4 Hz, SWA, 0.5–4 Hz, Theta, 4–8 Hz, slow spindle, 9–12 Hz, fast spindle, 12–15 Hz. Topographic maps are based on normalized spectral data.

In order to extract the time course of slow and fast spindle activity (instantaneous power), the raw signal was band-pass filtered in the respective spindle band (Chebyshev type II, 40 dB stop band attenuation, 2 Hz transition band) and the squared absolute value of its Hilbert transform was calculated. This procedure was used in the calculation of the event-related power and the measure for phase–amplitude coupling.

Relations between spindles and SOs

We used two measures for investigating the relation between slow oscillations and spindles in the 210 min stimulation interval. First, instantaneous spindle power within positive half-wave intervals was summed and normalized by the total duration of positive half-waves. Please note that this is based on all offline detected, not just evoked, slow oscillations.

Second, for the quantification of phase–amplitude coupling between fast spindles and slow oscillations we used the 'mean vector length' method described previously (Canolty *et al.*, 2006; Tort *et al.*, 2010). In short, the EEG signal $s(t)$ of a single channel was band-pass filtered from 12 to 15 Hz, Hilbert-transformed, squared and normalized by its SD to obtain the time course of instantaneous power, $A(t)$. The normalization is necessary to facilitate a comparison between conditions by eliminating the dependence on the overall power level. Similarly, $s(t)$ was band-pass filtered from 0.5 to 3.5 Hz, Hilbert-transformed and converted into a phase-signal $\varphi(t)$ by calculating the angle of the resulting complex-valued time series. $\varphi(t)$ assumes values in the interval $(-\pi, \pi)$ radians. The peak of the negative slow oscillation half-wave corresponds to $\varphi = \pi$ and the positive peak of the positive SO half-wave occurs at $\varphi = 0$. The mean vector length (M) is then defined as $M = |z|$ and the phase angle of the coupling is $\varphi^* = \mathrm{Im}\{\log(z)\}$, with $z = (1/T)\sum_{t=0}^{T} A(t)e^{i\varphi(t)}$. As we compare modulation indices across conditions, no further normalization is needed.

Time–frequency representation

Individual time–frequency representations were computed using EEGLAB's newtimef (Delorme & Makeig, 2004). First, trials of [−6, 6] s around first clicks were extracted and a linear trend removed (same as for event-related potentials). Second, a short-time Fourier transform using the Hanning window and 300 equally spaced, overlapping segments of 1 s length was applied to each trial. Third, the data were squared. Fourth, for each frequency the trial was divided by the average power across trials of the baseline interval [−2000, 0] ms. Fifth, trials were averaged and the logarithm taken. Sixth, *P*-values were obtained for each pixel using via a paired permutation *t*-test (stimulation vs. sham) with 4999 permutations using EEGLAB's statcond and corrected for multiple comparisons using the false discovery rate method for positively dependent test (Benjamini & Hochberg, 1995).

Statistical analysis

Statistical analysis was performed in MATLAB and R (R Development Core Team, 2008). Data are expressed as mean ± SD (or SEM when indicated). Normal distribution of data was assessed by Shapiro–Wilk test. Normalized EEG power was separately analyzed in the six frequency bands using two-way repeated measures analyses of variance (ANOVA) with the factors condition (stimulation vs. sham) and topography (Fp1, Fpz, Fp2, F7, F3, Fz, F4, F8, T3, C3, Cz, C4, T4, T5, P3, Pz, P4, T6, O1, Oz, O2). Additional repeated-measures factors were time and type, representing pre-stimulation, stimulation and post-stimulation period, and responder type respectively. Huynh–Feldt correction of degrees of freedom was applied where appropriate.

Running *P*-values in ERP plots were obtained using two-tailed Student's paired *t*-tests. *P*-values were corrected for multiple comparisons using the false discovery rate method for positively dependent tests (Benjamini & Hochberg, 1995).

Results

Twelve of 21 subjects reported to have noticed auditory stimulation during the night of which four perceived it as unpleasant. Eight subjects were clearly sensitive to stimulation, as they had arousals upon the beginning of a stimulation sequence and could only receive stimulation toward the end of the stimulation period.

The mean duration of stimulation epochs within the stimulation period was 49 ± 17 min for the stimulation condition and 47 ± 14 min for the sham condition. During this time 295 ± 119 (sham: 287 ± 105) click sequences were applied. The individually determined delay between first and second click was on average 942 ± 111 ms across subjects.

Event-related potentials, power and acute spindle response similar to auditory closed-loop stimulation

The EEG (averaged across subjects) time-locked to the first click revealed a series of strong slow oscillatory responses (Fig. 2A, top). The ability of the click sequences to evoke SO sequences is reflected in the event histogram of the delays (Fig. 2C). The probability to evoke a SO is similar for each click in a sequence, namely $P_{\text{click }1} = 0.39 \pm 0.16$, $P_{\text{click }2} = 0.37 \pm 0.15$ and $P_{\text{click }3} = 0.35 \pm 0.15$. However, the probability of a click sequence to evoke three consecutive SOs is relatively low but still significantly higher as compared to sham, ($P_{\text{Stimulation}}(SO_3|SO_2|SO_1) = 0.13 \pm 0.09$ vs. $P_{\text{Sham}}(SO_3|SO_2|SO_1) = 0.05 \pm 0.04$; $P < 0.001$).

Event-related fast spindle power (12–15 Hz) is depicted in Fig. 2A (middle). The first click triggered not only a large positive wave reflecting the depolarized component of the EEG (putative up state) around $t = 1$ s, but also a single strong response in spindle activity. In contrast, responses to the second and third clicks of a sequence at $t = 2$ s and $t = 3$ s are markedly lower. Furthermore, the baseline level of event-related fast spindle power is lower in the 'stimulation' condition than in the 'sham' condition.

Similarly, the mean level of event-related slow spindle power (9–12 Hz) is higher in sham (Fig. 2A, bottom). However, in contrast to fast spindle power, an increase in slow spindle power of similar magnitude can be seen after each click. This suggests that refractory processes play less of a role for slow than for fast spindles.

Next, we analyzed the EEG response to clicks separately for the cases where the first click in a sequence successfully evoked a KC and thus the succeeding click could be played into the next up-states as compared to when the click failed to do so ('KC' vs. 'no KC'). The event-related responses in Fig. 3 (top) clearly reflect the

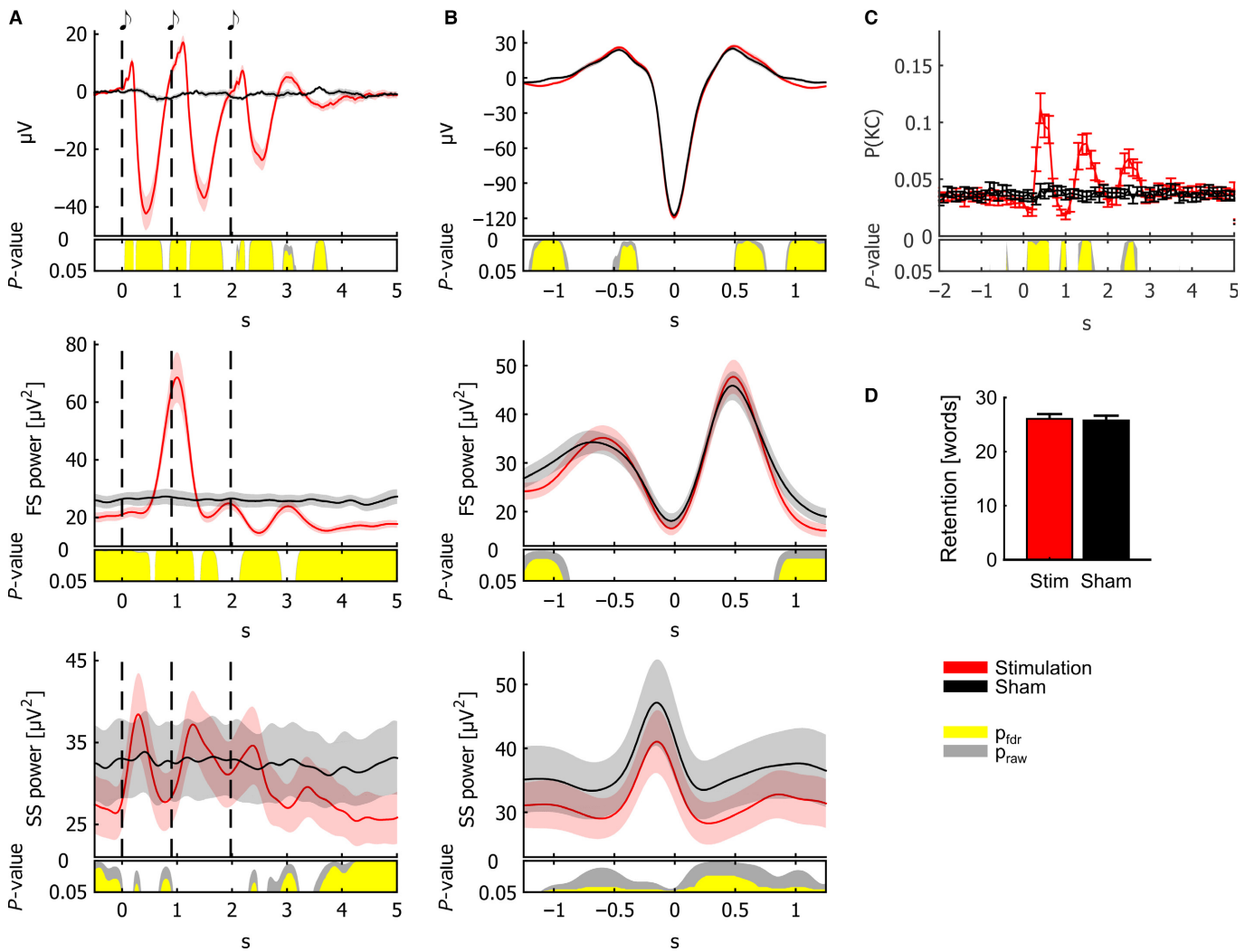

FIG. 2. No impact of open-loop auditory stimulation on memory consolidation despite effects on SOs and on spindle power. (A) Mean (±SEM) event-related response at Cz averaged for the wide-band EEG signal, (middle) fast spindle power (FS, 12–15 Hz) and (bottom) slow spindle power (SS, 9–12 Hz), time-locked to the first click of each sequence ($t = 0$ s), for stimulation (red) and sham (black) conditions. Vertical dashed lines indicate clicks. Time axis is adjusted for individual inter-stimulus intervals such that the second click occurs at 940 ms. Baseline has not been removed. See Fig. S2 for the event-related EMG response, indicating the absence of arousals after stimuli. (B) Mean (±SEM) of EEG signal (top), fast spindle power (middle) and slow spindle power (bottom), time-locked to the negative peak ($t = 0$ s) of all offline detected slow oscillations at Cz, for stimulation (red) and sham (black) conditions. Baseline correction was not conducted. (C) Mean (±SEM) event histogram of offline detected SO events at Fz during NREM sleep, time-locked to first click of a click sequence ($t = 0$ s) and restricted to the window [−2, 5] s, for the stimulation (red) and sham (black) conditions, averaged across subjects. (D) Mean (±SEM) difference between number of successfully recalled word pairs before and after sleep (retention) for the stimulation and sham conditions, averaged across subjects. (A,B,C) Bottom panels indicate significant differences between conditions (P-values): yellow – corrected using false discovery rate (P_{fdr}); gray – uncorrected (P_{raw}).

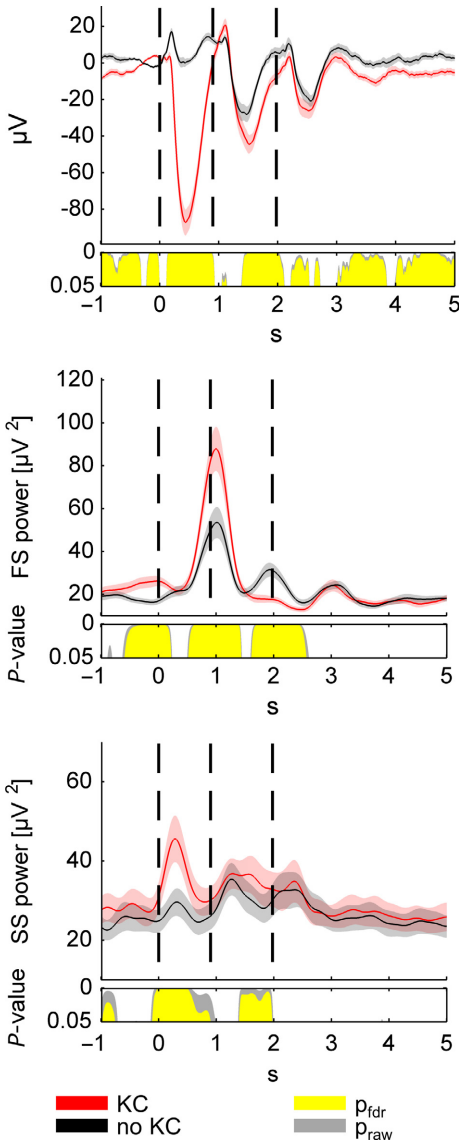

FIG. 3. EEG responses to click sequences: evoked KC vs. no KC after the first click. (Top) Mean (±SEM) event-related response at Cz averaged for the wide-band EEG signal, (middle) fast spindle power (FS, 12–15 Hz) and (bottom) slow spindle power (SS, 9–12 Hz), time-locked to the first click of each sequence (t = 0 s) for (red) successfully evoked KC after the first click and (black) missing KC after the first click. Note that after the second and third clicks, KCs may occur in both cases. Vertical dashed lines indicate clicks. Time axis is adjusted for individual inter-stimulus intervals such that the second click occurs at 940 ms. Baseline has not been removed. Bottom panels indicate significant differences between conditions (P-values): yellow – corrected using false discovery rate (P_{fdr}); gray – uncorrected (P_{raw}).

presence or absence of KCs. Notably, a significant increase in fast spindle power after the second click was present, regardless of whether the first click evoked a KC or not – the amplitude being larger in the 'KC' case (Fig. 3, middle). Furthermore, the amplitude of the fast spindle response following the second click is lower when the first click successfully evoked a KC. Slow spindles already show an increase upon the first click if it evoked a KC (Fig. 3, bottom).

In order to provide a more comprehensive overview of the frequency content of the EEG response to click sequences we calculated a time–frequency representation of the within-sequence intervals comparing stimulation and sham conditions (Fig. 4).

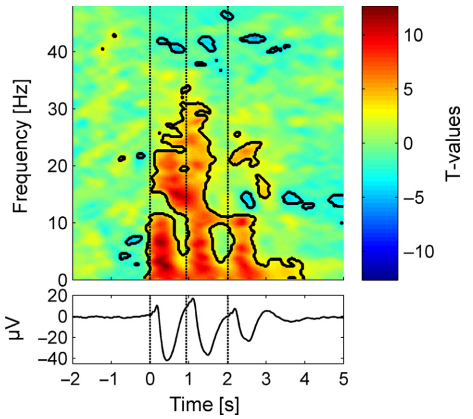

FIG. 4. Time–frequency representation of the response to click sequences at Cz. (Top) T-values (stimulation vs. sham) time-locked to the first click of each sequence (t = 0 s) in interval [−2, 5] s are shown. Black contours indicate regions with $P_{fdr} < 0.05$. (Bottom) Mean event-related response averaged for the wide-band EEG signal, time-locked to the first click of each sequence (t = 0 s), for the stimulation condition. (Top, Bottom) Vertical dashed lines indicate clicks. Time axis is adjusted for individual inter-stimulus intervals such that the second click occurs at 940 ms.

Next, we investigated how the morphology of slow oscillation events was influenced by the stimulation. For this, we averaged all offline detected slow oscillation events time-locked to the negative peak of their negative half-wave (Fig. 2B, top). This revealed that the amplitude of the main negative half-wave of the SO (t = 0 s, P_{fdr} = 0.17) was unaffected by stimulation. Open-loop stimulation, however, increased the amplitudes of positive half-waves (at $t = \pm 0.5$ s, $P_{fdr} < 0.01$) and negative half-waves (at $t = \pm 1$ s, $P_{fdr} < 0.01$). This may reflect the greater occurrence of SO trains induced by the click sequences, as indicated by the event histogram in Fig. 2C.

Differential effects on slow-wave power and spindle power

Stimulation had opposite effects on SOs and spindles. While power in SO, delta and SWA bands was increased throughout NREM sleep of the stimulation epochs ($F_{1,20}$ = 7.6, P = 0.012; $F_{1,20}$ = 4.5, P = 0.047; $F_{1,20}$ = 7.7, P = 0.012), power in slow and fast spindle bands decreased during this time ($F_{1,20}$ = 17.6, $P < 0.001$; $F_{1,20}$ = 25.1, $P < 0.001$; see Fig. 5A, bottom row). The effect on SO power was strongest in frontal regions and exhibited a lateralization to the right hemisphere. Slow spindle power was altered mainly at central leads and fast spindle power at centro-parietal leads (Fig. 5, top row).

In addition to the stimulation period, we evaluated EEG power during N2 epochs between sleep onset and beginning of the stimulation (pre-stimulation period) and NREM sleep epochs of the post-stimulation period (see Fig. 1B for definitions). As could be expected, power in N2 epochs preceding the stimulation period did not differ between conditions ($P > 0.24$ for all ANOVA condition main effects and condition × topography interaction). Hence, we can rule out that the changes observed during the stimulation period are due to a preexisting baseline offset.

During post-stimulation NREM sleep epochs power in SO, delta and SWA bands was also increased, despite absence of stimulation. The presence of this effect depended on electrode site (condition × topography interaction: SO, $F_{20,400}$ = 3.64, P = 0.036; delta, $F_{20,400}$ = 3.41, P = 0.041; SWA, $F_{20,400}$ = 3.85, P = 0.028). The suppression of slow spindle power also extended beyond acute

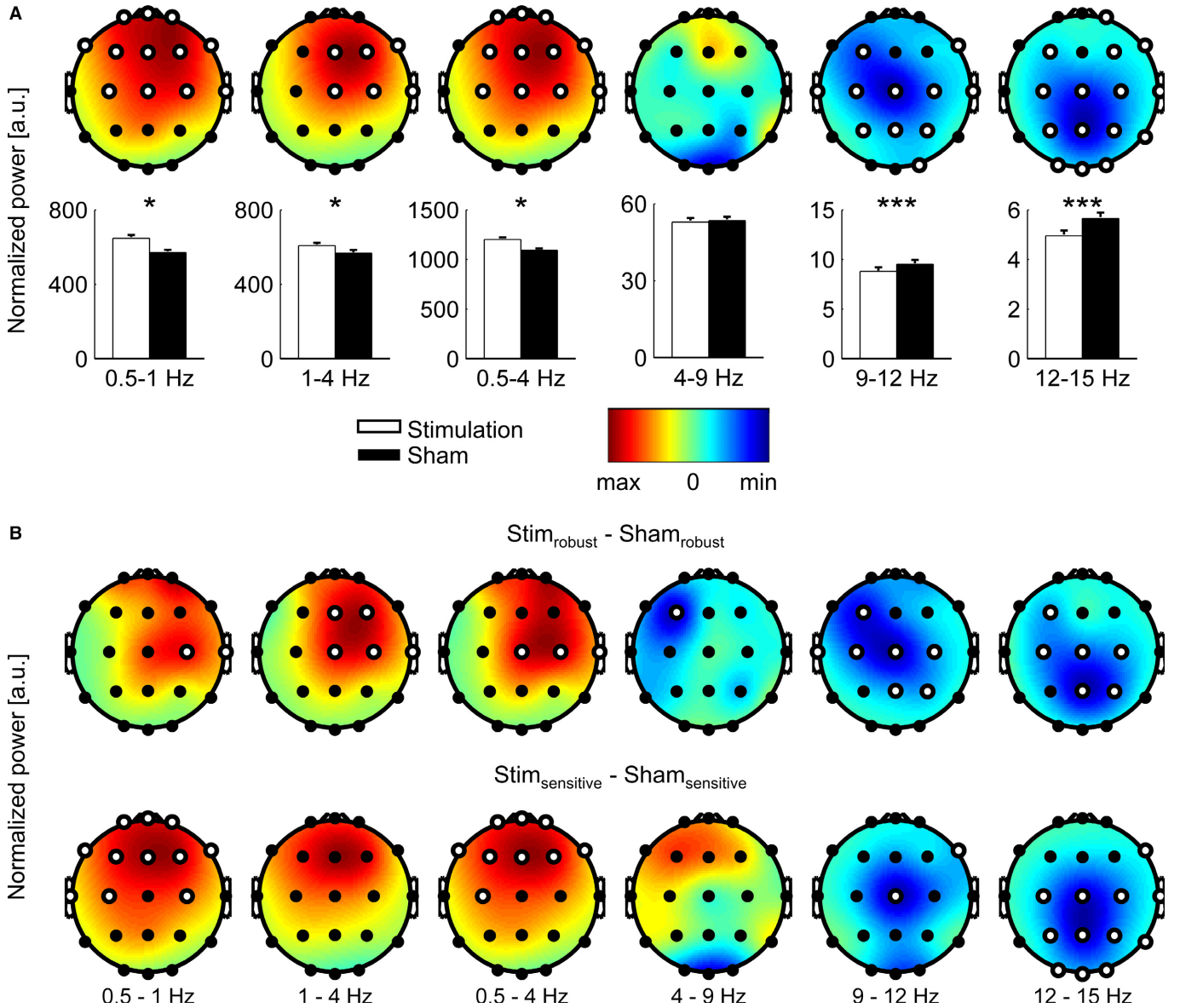

FIG. 5. Topographical distribution of stimulation efficiency. (A, top row) Difference (stimulation–sham) of normalized spectral power in SO, delta, SWA, theta, slow spindle and fast spindle band for the 210 min stimulation period. Electrode locations with a significant difference ($P_{fdr} < 0.05$, paired *t*-test, corrected for multiple comparisons) are depicted as white circles. (A, bottom row) Mean (±SEM) of normalized spectral power averaged over all subjects and all electrodes, for the stimulation (white) and sham (black bars) conditions. Frequency bands apply to top and bottom rows. (B) Same as in A, but for (top) robust and (bottom) sensitive responders. *$P < 0.05$, ***$P < 0.001$.

stimulation into the post-stimulation NREM sleep epochs (condition main effect: $F_{20,400} = 4.44$, $P = 0.048$). However, *post hoc t*-tests did not reveal any significant effects however, neither for any electrode site nor for any frequency band ($P_{fdr} > 0.18$ at all electrodes). Figure 6 summarizes therefore the overall time course of power across the three periods of nocturnal sleep in the different frequency bands. Neither baseline nor rebound effects are evident for any of the six frequency bands.

Within-sequence interval and inter-sequence interval spindle power

To further characterize the decrease in spindle power within the stimulation period, we calculated separately mean spindle power for the within-sequence intervals and inter-sequence intervals (see Fig. 1B for definitions). The results are given in Fig. 7A (top row). The decrease in fast and slow spindle power is confined to the time between click sequences. Spindle power in the inter-sequence intervals is lower in the stimulation than the sham condition (fast spindles: 19.1 ± 7 μV^2 vs. 25.8 ± 9.9 μV^2, $P < 0.001$; slow spindles: 25.6 ± 14.8 μV^2 vs. 32.3 ± 20.6 μV^2, $P < 0.001$), whereas power levels of within-sequence intervals are similar ($P > 0.31$). For the stimulation condition only spindle power in within-sequence intervals is higher than in inter-sequence intervals (fast spindles: 26.1 ± 9.1 μV^2 vs. 19.1 ± 7 μV^2, $P < 0.001$; slow spindles: 31.2 ± 17.5 μV^2 vs. 25.6 ± 14.8 μV^2, $P < 0.001$).

Surprisingly, within the stimulation period fast spindle power during positive half-waves of SOs was not affected (36.1 ± 11.8 μV^2 vs. 35.7 ± 11.9 μV^2, $P = 0.83$), but power decreased in the case of slow spindles (30.4 ± 15.4 μV^2 vs. 35.0 ± 21.3 μV^2, $P = 0.012$;

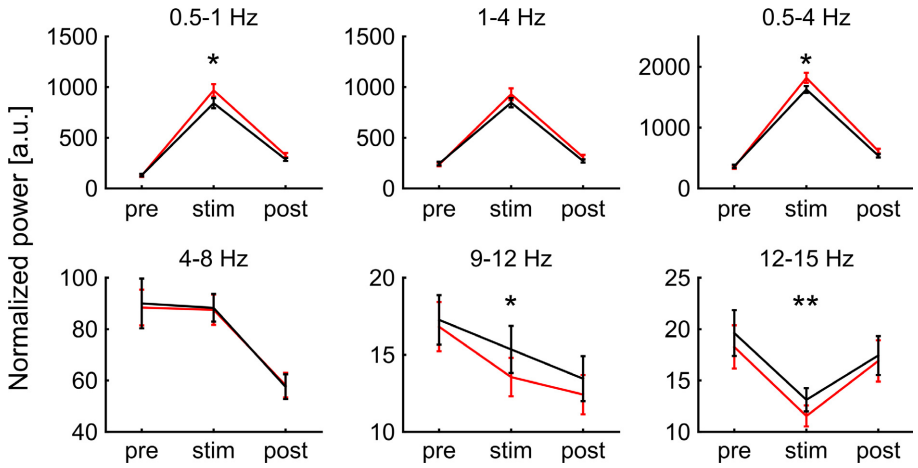

FIG. 6. Spectral power at Cz across the night. Mean (±SEM) of normalized spectral power over course of night at Cz averaged over subjects, for stimulation (red) and sham (black) conditions. 'pre': N2 epochs of the pre-stimulation period. 'stim': NREM sleep epochs with clicks during the 210-min stimulation period, i.e. the stimulation epochs. 'post': NREM sleep epochs after stimulation period, i.e. the post-stimulation period. $*P_{fdr} < 0.05$, $**P_{fdr} < 0.01$, paired *t*-test.

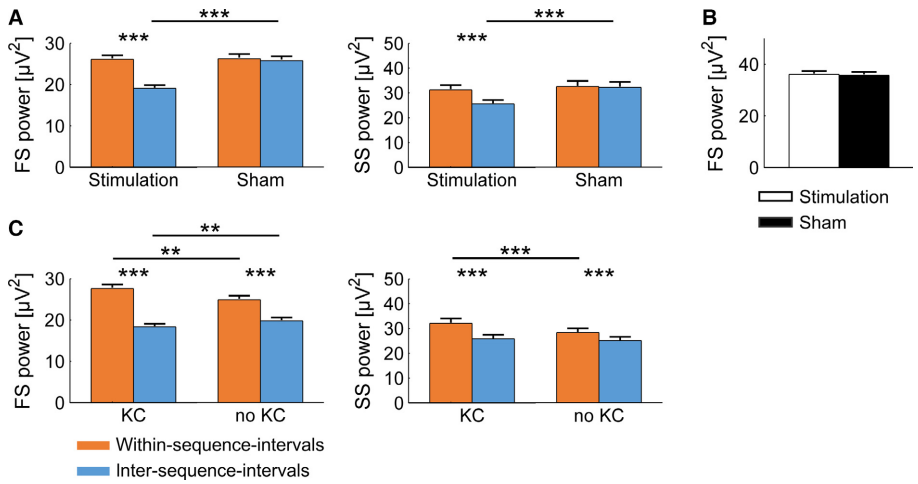

FIG. 7. Stimulation-related decrease in spindle power. (A) Mean (±SEM) of fast spindle power (left) and slow spindle power (right) in within-sequence intervals (red) and inter-sequence intervals (blue) for stimulation and sham conditions. See Fig. 1 for the definition of the intervals. (B) Mean (±SEM) of fast spindle power during positive half-waves of offline detected SOs in the 210-min stimulation period for stimulation (white) and sham (black) conditions. (C) Separately for the stimulation condition only, mean (±SEM) of fast spindle power (left) and slow spindle power (right) in within-sequence intervals (red) and inter-sequence intervals (blue) for sequences where the first click successfully evoked a KC ('KC') as compared to click sequences where it did not ('no KC'). (A, B, C) Power is calculated from time series of instantaneous power, without normalization. $*P < 0.05$, $**P < 0.01$, $***P < 0.001$.

depicted in Fig. 2B middle/bottom and Fig. 7B, see 'Relations between spindles and SOs' in Materials and methods).

This analysis is closely related to the mean vector length, *M*, a common measure for quantification of phase–amplitude coupling. As we observe that spindle power in positive half-waves of SOs remains similar across conditions despite an overall decrease in spindle power in the stimulation condition, we expect the mean vector length to be higher in the stimulation condition. Indeed, this is what happens (stimulation: $M = 0.09 \pm 0.03$, sham: $M = 0.07 \pm 0.03$, $P = 0.004$). The phase at which fast spindles are coupled strongest to the slow oscillation does not differ between conditions (stimulation: $\varphi^* = -0.24 \pm 0.28$, sham: $\varphi^* = -0.19 \pm 0.30$, confidence interval CI = [−0.11, 0.02], paired sample test for angular data; Zar, 1999).

We also repeated the analysis separately for the sequences where the first click successfully evoked a KC and for those where it did not. The spindle power in within-sequence and inter-sequence intervals for the 'KC' and 'no KC' cases are depicted in Fig. 7C. A suppression of spindle power in the inter-sequence intervals as compared to the within-sequence intervals is present in both the 'KC' as well as 'no KC' group for fast and slow spindles. When the first click successfully evoked a KC, however, power in within-sequence intervals was higher for fast and slow spindles. In addition, for fast spindles the decrease in power in the inter-sequence interval was also more pronounced in the KC group.

Open-loop stimulation does not improve memory consolidation

Open-loop auditory stimulation did not affect overnight retention, i.e. the difference in the number of words recalled when tested after sleep and the number recalled at learning before sleep, compared to sham (26.0 ± 8.3 vs. 25.8 ± 1.8 word pairs, $P = 0.89$, see Fig. 2D). Learning performance before sleep did not differ significantly between conditions (stimulation vs. sham: 61.3 ± 20.6 vs. 62.3 ± 19.4 word pairs, $P = 0.74$).

Control measures of sleep quality, mood and tiredness (SF-A, PANAS, SSS) were comparable across conditions (all $P > 0.13$). Similarly, the measures of general cognitive ability (DST, RWT) did

TABLE 1. Overview of control measures

Test	Stimulation		Sham		*P*-value
	Evening	Morning	Evening	Morning	
SF-A	n.a.	3.2 ± 0.5	n.a.	3.2 ± 0.6	0.8*
SSS	4.3 ± 1.1	3.5 ± 0.9	4.2 ± 1.1	3.3 ± 1.0	0.75**
PANAS (P)	21.1 ± 5.4	21.4 ± 6.5	21.1 ± 4.3	23.6 ± 6.2	0.12**
PANAS (N)	11.8 ± 3.3	11.4 ± 2.2	11.7 ± 2.7	11.5 ± 2.5	0.59**
PVT	309.0 ± 27.0	305.0 ± 21.3	304.3 ± 24.6	307.6 ± 21.5	0.05**
DST	n.a.	20.9 ± 4.1	n.a.	21.5 ± 4.8	0.57*
RWT	n.a.	37.3 ± 8.6	n.a.	36.2 ± 8.5	0.45*

Mean ± SD, *paired *t*-test, **two-way ANOVA (condition × time).

not exhibit significant differences ($P > 0.12$, see Table 1). The PVT differs between conditions ($P = 0.05$, interaction condition × time, see also Table 1) due to a baseline difference in the evening, in which performance in the sham condition was slightly better than in the stimulation condition ($PVT_{ev,Stim} = 309.0 \pm 27.0$ ms, $PVT_{ev,Sham} = 304.3 \pm 24.6$ ms).

Sleep architecture

There were no significant differences in sleep architecture between conditions for the full night, except for N3, in which subjects spent more time during the 'stimulation' condition ($P = 0.04$, Wilcoxon signed-rank test, see Table 2). However, analysis of the N3 duration in the stimulation period and the remaining period of nocturnal sleep with a two-way ANOVA (factors time and condition), failed to reach significance (condition: $F_{1,20} = 3.4$, $P = 0.08$; time × condition: $F_{1,20} = 0.353$, $P = 0.56$). We also failed to find any significant correlation for either condition between overnight retention of word pairs and time (percentage) spent in individual sleep stages or in EEG power within the six frequency bands at electrode Cz using Pearson correlations after correcting for multiple comparisons ($P > 0.12$) (Supporting Information Table S2).

Comparison of 'robust' and 'sensitive' responders

Eight of the 21 subjects had frequent arousals in the beginning of the night, possibly linked to stimulation. Therefore, most of the stimuli occurred toward the end of the 210 min stimulation period. It has been reported that reactivation processes during sleep seem to be strongest at early portions of NREM sleep (Bendor & Wilson, 2012). Furthermore, SOs appear to be more global during early fractions of sleep (Nir *et al.*, 2011). Hence, we investigated whether the timing issue had an effect on memory consolidation and oscillatory activity associated with auditory stimulation.

We split the participants into the two groups 'robust' (13 subjects) and 'sensitive' (eight subjects). A three-way ANOVA with factors time, condition and responder type, however, did not reveal any significant influence of responder type on the overnight consolidation of word pairs (time × condition × type: $F_{1,19} = 0.373$, $P = 0.55$).

Interestingly, the efficacy of the stimulation in the SO and SWA bands indeed differed between the groups, revealing a stronger impact on the sensitive responders (SO, main effect condition: $F_{1,19} = 12.2$, $P = 0.002$, interaction condition × topography × type: $F_{1,19} = 5.0$, $P = 0.001$; SWA, main effect condition: $F_{1,19} = 10.6$, $P = 0.004$, interaction condition × topography × type: $F_{1,19} = 3.6$, $P = 0.005$). There were no significant differences between responder types in any other frequency band. Figure 5B depicts the topographies of both responder types. The changes in slow and fast spindle activity are independent of responder type.

Furthermore, we re-analyzed separately for robust and sensitive responders spindle power in within-sequence and inter-sequence intervals and fast spindle power during putative slow oscillation up states. The pattern of results does not differ between the groups (Supporting Information Fig. S1).

TABLE 2. Sleep architecture

Parameter	Stimulation	Sham	*P*-value
Whole night			
SPT (min)	398.8 ± 8.9	401.0 ± 6.3	0.67
W (%)	2.2 ± 0.7	1.9 ± 0.5	0.74
N1 (%)	7.6 ± 0.9	8.2 ± 0.9	0.41
N2 (%)	46.8 ± 1.5	48.3 ± 1.3	0.24
N3 (%)	25.9 ± 1.8	23.5 ± 1.5	0.04
REM (%)	17.5 ± 0.9	18.0 ± 1.0	0.88
MA (%)	7.4 ± 0.5	7.4 ± 0.6	0.85
Stimulation period			
W (%)	1.7 ± 0.8	1.3 ± 0.6	0.45
N1 (%)	4.4 ± 0.8	4.5 ± 0.7	0.45
N2 (%)	39.7 ± 2.5	41.9 ± 2.0	0.15
N3 (%)	46.5 ± 3.2	45.1 ± 2.6	0.74
REM (%)	7.6 ± 1.3	7.2 ± 1.2	0.71
MA (%)	7.2 ± 0.7	7.0 ± 0.7	0.99
Post-stimulation period			
W (%)	2.5 ± 1.1	1.7 ± 0.4	0.27
N1 (%)	7.8 ± 1.1	8.4 ± 1.0	0.64
N2 (%)	49.6 ± 1.8	52.3 ± 1.5	0.24
N3 (%)	15.0 ± 2.1	11.4 ± 1.5	0.10
REM (%)	25.1 ± 1.4	26.3 ± 1.6	0.39
MA (%)	7.5 ± 0.6	7.9 ± 0.7	0.71

Mean (±SEM) of time spent in different sleep stages during the whole night, 210-min stimulation period and post-stimulation period for stimulation and sham conditions. Wilcoxon's signed-rank test was used for *P*-values. SPT, sleep period time (first N1 until awakening); W, wake; N1 and N2, non-REM sleep stages 1 and 2; N3, slow-wave sleep; REM, rapid eye movement sleep; MA, movement arousals.

Discussion

In this study, we investigated whether it is possible to improve the overnight consolidation of declarative memories with a modified version of the auditory closed-loop stimulation paradigm (Ngo *et al.*, 2013, 2015), which is phase independent. We found that open-loop stimulation with sequences of three clicks evoked SOs, lead to an increase in SO power and a decrease in slow and fast

spindle power, but did not alter the overnight retention of word pairs. Similar to the closed-loop stimulation, we found that only the first click in a sequence evoked a strong spindle response. We attribute this effect to the mechanisms of endogenous spindle termination and the refractory period between spindles. This has been ascribed to (1) an upregulation of the hyperpolarization-activated nonspecific cation current, I_h, in thalamocortical cells (Lüthi & McCormick, 1998) or (2) depolarization in thalamocortical cells by cortical feedback which is no longer phase-locked with inhibitory postsynaptic potentials (Bonjean *et al.*, 2011). Both mechanisms prevent the de-inactivation of the low-threshold T-type Ca^{2+} channels involved in spindle initiation.

Notably, open-loop stimulation caused an overall decrease in spindle power in the stimulation period, whereas this has not been reported for the phase-dependent version (Ngo *et al.*, 2013, 2015).

The observed decrease in spindle power suggests that open-loop stimulation disturbs ongoing endogenous spindle generation. This has also been found with electric stimulation in the lateroposterior thalamic nucleus of anesthetized cats, where a locally induced spindle, out of phase with the endogenous rhythm, prevented the occurrence of the next endogenous spindle in the same location (Contreras *et al.*, 1997). In order to generate spindles, neurons in the reticular nucleus have to be sufficiently hyperpolarized, so that low-threshold Ca^{2+} currents can deinactivate and initiate bursting (Astori *et al.*, 2011; Lee *et al.*, 2013). On the other hand, a much increased level of hyperpolarization prevents spindle oscillations and instead gives rise to thalamic delta oscillations (Nunez *et al.*, 1992). Auditory stimulation was shown to have a net excitatory, i.e. depolarizing, effect on its thalamic targets (Yu *et al.*, 2004). Thus, open-loop stimulation might reduce spindle power by preventing a repolarization of the membrane potential in thalamic nuclei. The main advantage of closed-loop stimulation over open-loop stimulation is that the first click by design always occurs during an up state. In this situation, many thalamic nuclei are already depolarized due to the cortical up state (Sheroziya & Timofeev, 2014) and excitatory sensory inputs may cause only little additional depolarization relative to a hyperpolarized state. Hence, auditory closed-loop stimulation is less likely to disturb the endogenous spindle-generating mechanisms.

A further comparative observation to the study by Ngo *et al.* (2013) is that clicks were always preceded by an endogenous SO, i.e. were preceded by an endogenous spindle with high probability (Mölle *et al.*, 2002; Steriade, 2006). Surprisingly, in Ngo *et al.* (2013), the spindle response following the first click was even stronger than that of the preceding endogenous spindle. This suggests that there is no absolute refractory period of the spindle generating network, as also noted in Contreras *et al.* (1997). There, strong stimuli could trigger a spindle at any time, even during an ongoing spindle sequence, because only a fraction of neurons participated in each spindle (Contreras & Steriade, 1996; Destexhe *et al.*, 1996). Combined MEG-EEG recordings suggest that spindles are only visible in the EEG when they involve larger parts of the cortex (Dehghani *et al.*, 2011).

Thus, the fact that an external auditory click can evoke a strong spindle response directly after an endogenous spindle event indicates that it recruits otherwise silent neurons into a spindle oscillation and/or increases thalamic synchrony.

Several studies report a positive correlation between spindle power and overnight retention (Gais *et al.*, 2002; Schabus *et al.*, 2004; Fogel & Smith, 2011; Tamminen *et al.*, 2013). Interestingly, in the present study, memory performance of the stimulation night was similar to that of the sham night, although power in the slow and fast spindle band was markedly decreased throughout the stimulation period and no rebound of SO or spindle power occurred in the post-stimulation period. One could argue that, albeit statistically significant, the effect was not strong enough to influence the behavioral outcome. Alternatively, it could be that specific aspects of spindle activity are responsible for its efficacy with respect to memory consolidation and those are not altered by open-loop stimulation. In the present study, fast spindle power during positive half-waves of SOs remained at the same level as in the sham condition and the reduction in fast spindle power is restricted to the intervals between click sequences only. Thus, the relative timing of spindles and SOs, which is critical for memory consolidation (Mölle *et al.*, 2009; Cox *et al.*, 2012; Ngo *et al.*, 2013; Niknazar *et al.*, 2015), was mostly not perturbed during the stimulation period.

Finally, others have demonstrated that SO and spindle rhythms by themselves may induce long-term plasticity and therefore may independently contribute to memory consolidation (Rosanova & Ulrich, 2005; Chauvette *et al.*, 2012). Hence, in the present study, a positive effect of increased SO power on memory consolidation might offset a detrimental effect of decreased spindle power. However, at least in humans enhancing slow-wave activity alone by pharmacological means (without increasing sleep spindle activity) does not improve overnight memory consolidation (Feld *et al.*, 2013). Also, benzodiazepines which are known to enhance sleep spindle activity and suppress slow-wave activity (Brunner *et al.*, 1991; Arbon *et al.*, 2015) have inconsistent effects on memory consolidation (Meléndez *et al.*, 2005; Mednick *et al.*, 2013; Hall-Porter *et al.*, 2014). Thus, at least some findings indicate that neither enhancing slow-wave nor spindle activity alone might be sufficient to enhance later memory performance. In contrast, increasing slow-wave and spindle activity simultaneously has shown a benefit (Marshall *et al.*, 2006; Ngo *et al.*, 2013, 2015).

Conflicts of interest

The authors declare no competing financial interests.

Supporting Information

Additional supporting information can be found in the online version of this article:
Table S1. Behavioral data.
Table S2. Correlations of memory performance with sleep parameters.
Fig. S1. Stimulation-related decrease in spindle power: robust vs. sensitive responders.
Fig. S2. EMG response to click sequences.

Acknowledgements

We thank the anonymous reviewers for their valuable suggestions and contributions. This work was supported by the US-German Collaboration in Computational Neuroscience (BMBF grant 01GQ1008) and the Deutsche Forschungsgemeinschaft (SFB-TR 654, Graduate School 235 and DFG SPP1665).

Abbreviations

DST, Digit Span Test; EEG, electroencephalogram; FS, fast spindle; NREM, non-rapid eye movement; PAL, paired-associate learning; PANAS, Positive and Negative Affect Schedule; PVT, psychomotor vigilance test; REM, rapid eye movement; RWT, Regensburg Word Fluency Test; SF-A, Sleep Questionnaire A; SO, slow oscillation; SS, slow spindle; SSS, Stanford Sleepiness Scale.

References

Anderer, P., Klösch, G., Gruber, G., Trenker, E., Pascual-Marqui, R.D., Zeitlhofer, J., Barbanoj, M.J., Rappelsberger, P. *et al.* (2001) Low-resolution brain electromagnetic tomography revealed simultaneously active frontal and parietal sleep spindle sources in the human cortex. *Neuroscience*, **103**, 581–592.

Arbon, E.L., Knurowska, M. & Dijk, D.-J. (2015) Randomised clinical trial of the effects of prolonged-release melatonin, temazepam and zolpidem on slow-wave activity during sleep in healthy people. *J. Psychopharmacol.*, **29**, 764–776.

Aschenbrenner, S., Tucha, O. & Lange, K. (2000) *Regensburg Word Fluency Test*. Hogrefe, Göttingen.

Astori, S., Wimmer, R.D., Prosser, H.M., Corti, C., Corsi, M., Liaudet, N., Volterra, A., Franken, P. *et al.* (2011) The CaV3.3 calcium channel is the major sleep spindle pacemaker in thalamus. *Proc. Natl. Acad. Sci. USA*, **108**, 13823–13828.

Bastien, C. & Campbell, K. (1994) Effects of rate of tone-pip stimulation on the evoked K-complex. *J. Sleep Res.*, **3**, 65–72.

Bastien, C.H., Crowley, K.E. & Colrain, I.M. (2002) Evoked potential components unique to non-REM sleep: relationship to evoked K-complexes and vertex sharp waves. *Int. J. Psychophysiol.*, **46**, 257–274.

Bendor, D. & Wilson, M.A. (2012) Biasing the content of hippocampal replay during sleep. *Nat. Neurosci.*, **15**, 1439–1444.

Benjamini, Y. & Hochberg, Y. (1995) Controlling the false discovery rate: a practical and powerful approach to multiple testing. *J. Roy. Stat. Soc. B Met.*, **57**, 289–300.

Bonjean, M., Baker, T., Lemieux, M., Timofeev, I., Sejnowski, T. & Bazhenov, M. (2011) Corticothalamic feedback controls sleep spindle duration *in vivo*. *J. Neurosci.*, **31**, 9124.

Brunner, D.P., Dijk, D.-J., Münch, M. & Borbély, A.A. (1991) Effect of zolpidem on sleep and sleep EEG spectra in healthy young men. *Psychopharmacology*, **104**, 1–5.

Canolty, R.T., Edwards, E., Dalal, S.S., Soltani, M., Nagarajan, S.S., Kirsch, H.E., Berger, M.S., Barbaro, N.M. *et al.* (2006) High gamma power is phase-locked to theta oscillations in human neocortex. *Science*, **313**, 1626–1628.

Chauvette, S., Seigneur, J. & Timofeev, I. (2012) Sleep oscillations in the thalamocortical system induce long-term neuronal plasticity. *Neuron*, **75**, 1105–1113.

Clemens, Z., Mölle, M., Eross, L., Barsi, P., Halasz, P. & Born, J. (2007) Temporal coupling of parahippocampal ripples, sleep spindles and slow oscillations in humans. *Brain*, **130**, 2868–2878.

Contreras, D. & Steriade, M. (1995) Cellular basis of EEG slow rhythms: a study of dynamic corticothalamic relationships. *J. Neurosci.*, **15**, 604–622.

Contreras, D. & Steriade, M. (1996) Spindle oscillation in cats: the role of corticothalamic feedback in a thalamically generated rhythm. *J. Physiol.*, **490**, 159–179.

Contreras, D., Destexhe, A., Sejnowski, T.J. & Steriade, M. (1997) Spatiotemporal patterns of spindle oscillations in cortex and thalamus. *J. Neurosci.*, **17**, 1179–1196.

Cox, R., Hofman, W.F. & Talamini, L.M. (2012) Involvement of spindles in memory consolidation is slow wave sleep-specific. *Learn. Memory*, **19**, 264–267.

David, F., Schmiedt, J.T., Taylor, H.L., Orban, G., Di Giovanni, G., Uebele, V.N., Renger, J.J., Lambert, R.C. *et al.* (2013) Essential thalamic contribution to slow waves of natural sleep. *J. Neurosci.*, **33**, 19599–19610.

Dehghani, N., Cash, S.S. & Halgren, E. (2011) Emergence of synchronous EEG spindles from asynchronous MEG spindles. *Hum. Brain Mapp.*, **32**, 2217–2227.

Delorme, A. & Makeig, S. (2004) EEGLAB: an open source toolbox for analysis of single-trial EEG dynamics including independent component analysis. *J. Neurosci. Meth.*, **134**, 9–21.

Destexhe, A. & Sejnowski, T.J. (2003) Interactions between membrane conductances underlying thalamocortical slow-wave oscillations. *Physiol. Rev.*, **83**, 1401–1453.

Destexhe, A., Bal, T., McCormick, D.A. & Sejnowski, T.J. (1996) Ionic mechanisms underlying synchronized oscillations and propagating waves in a model of ferret thalamic slices. *J. Neurophysiol.*, **76**, 2049–2070.

Development Core Team, R. (2008) R: a language and environment for statistical computing. R Foundation for Statistical Computing, Vienna, Austria.

Ego-Stengel, V. & Wilson, M.A. (2010) Disruption of ripple-associated hippocampal activity during rest impairs spatial learning in the rat. *Hippocampus*, **20**, 1–10.

Feld, G.B., Wilhelm, I., Ma, Y., Groch, S., Binkofski, F., Mölle, M. & Born, J. (2013) Slow wave sleep induced by GABA agonist tiagabine fails to benefit memory consolidation. *Sleep*, **36**, 1317.

Fogel, S.M. & Smith, C.T. (2011) The function of the sleep spindle: a physiological index of intelligence and a mechanism for sleep-dependent memory consolidation. *Neurosci. Biobehav. R.*, **35**, 1154–1165.

Gais, S., Mölle, M., Helms, K. & Born, J. (2002) Learning-dependent increases in sleep spindle density. *J. Neurosci.*, **22**, 6830–6834.

Girardeau, G., Benchenane, K., Wiener, S.I., Buzsáki, G. & Zugaro, M.B. (2009) Selective suppression of hippocampal ripples impairs spatial memory. *Nat. Neurosci.*, **12**, 1222–1223.

Görtelmeyer, R. (1981) *Schlaffragebogen SF-A und SF-B. Internationale Skalen für Psychiatrie*. Beltz, Weinheim.

Hall-Porter, J.M., Schweitzer, P.K., Eisenstein, R.D., Ahmed, H.A.H. & Walsh, J.K. (2014) The effect of two benzodiazepine receptor agonist hypnotics on sleep-dependent memory consolidation. *J. Clin. Sleep Med.*, **10**, 27.

Hoddes, E., Zarcone, V., Smythe, H., Phillips, R. & Dement, W.C. (1973) Quantification of sleepiness: a new approach. *Psychophysiology*, **10**, 431–436.

Iber, C., Ancoli-Israel, S., Chesson, A.L. & Quan, S.F. (2007) *The AASM Manual for the Scoring of Sleep and Associated Events: Rules, Terminology and Technical Specifications*. American Academy of Sleep Medicine, Westchester.

Kandel, A. & Buzsaki, G. (1997) Cellular-synaptic generation of sleep spindles, spike-and-wave discharges, and evoked thalamocortical responses in the neocortex of the rat. *J. Neurosci.*, **17**, 6783–6797.

Lee, J., Song, K., Lee, K., Hong, J., Lee, H., Chae, S., Cheong, E. & Shin, H.-S. (2013) Sleep spindles are generated in the absence of T-type calcium channel-mediated low-threshold burst firing of thalamocortical neurons. *Proc. Natl. Acad. Sci. USA*, **110**, 20266–20271.

Lüthi, A. & McCormick, D.A. (1998) Periodicity of thalamic synchronized oscillations: the role of Ca^{2+}-mediated upregulation of I_h. *Neuron*, **20**, 553–563.

Marshall, L., Helgadottir, H., Molle, M. & Born, J. (2006) Boosting slow oscillations during sleep potentiates memory. *Nature*, **444**, 610–613.

Mednick, S.C., McDevitt, E.A., Walsh, J.K., Wamsley, E., Paulus, M., Kanady, J.C. & Drummond, S.P.A. (2013) The critical role of sleep spindles in hippocampal-dependent memory: a pharmacology study. *J. Neurosci.*, **33**, 4494–4504.

Meléndez, J., Galli, I., Boric, K., Ortega, A., Zuñiga, L., Henríquez-Roldán, C.F. & Cárdenas, A.M. (2005) Zolpidem and triazolam do not affect the nocturnal sleep-induced memory improvement. *Psychopharmacology*, **181**, 21–26.

Mölle, M. & Born, J. (2011) Slow oscillations orchestrating fast oscillations and memory consolidation. *Prog. Brain Res.*, **193**, 93–110.

Mölle, M., Marshall, L., Gais, S. & Born, J. (2002) Grouping of spindle activity during slow oscillations in human non-rapid eye movement sleep. *J. Neurosci.*, **22**, 10941.

Mölle, M., Yeshenko, O., Marshall, L., Sara, S.J. & Born, J. (2006) Hippocampal sharp wave-ripples linked to slow oscillations in rat slow-wave sleep. *J. Neurophysiol.*, **96**, 62–70.

Mölle, M., Eschenko, O., Gais, S., Sara, S.J. & Born, J. (2009) The influence of learning on sleep slow oscillations and associated spindles and ripples in humans and rats. *Eur. J. Neurosci.*, **29**, 1071–1081.

Mölle, M., Bergmann, T.O., Marshall, L. & Born, J. (2011) Fast and slow spindles during the sleep slow oscillation: disparate coalescence and engagement in memory processing. *Sleep*, **34**, 1411–1421.

Ngo, H.-V.V., Martinetz, T., Born, J. & Mölle, M. (2013) Auditory closed-loop stimulation of the sleep slow oscillation enhances memory. *Neuron*, **78**, 545–553.

Ngo, H.-V.V., Miedema, A., Faude, I., Martinetz, T., Mölle, M. & Born, J. (2015) Driving sleep slow oscillations by auditory closed-loop stimulation —a self-limiting process. *J. Neurosci.*, **35**, 6630–6638.

Niknazar, M., Krishnan, G.P., Bazhenov, M. & Mednick, S.C. (2015) Coupling of thalamocortical sleep oscillations are important for memory consolidation in humans. *PLoS One*, **10**, e0144720.

Nir, Y., Staba, R.J., Andrillon, T., Vyazovskiy, V.V., Cirelli, C., Fried, I. & Tononi, G. (2011) Regional slow waves and spindles in human sleep. *Neuron*, **70**, 153–169.

Nunez, A., Curró Dossi, R., Contreras, D. & Steriade, M. (1992) Intracellular evidence for incompatibility between spindle and delta oscillations in thalamocortical neurons of cat. *Neuroscience*, **48**, 75–85.

Peyrache, A., Battaglia, F.P. & Destexhe, A. (2011) Inhibition recruitment in prefrontal cortex during sleep spindles and gating of hippocampal inputs. *Proc. Natl. Acad. Sci. USA*, **108**, 17207–17212.

Rasch, B. & Born, J. (2013) About sleep's role in memory. *Physiol. Rev.*, **93**, 681–766.

Rosanova, M. & Ulrich, D. (2005) Pattern-specific associative long-term potentiation induced by a sleep spindle-related spike train. *J. Neurosci.*, **25**, 9398–9405.

Schabus, M., Gruber, G., Parapatics, S., Sauter, C., Klosch, G., Anderer, P., Klimesch, W., Saletu, B. *et al.* (2004) Sleep spindles and their significance for declarative memory consolidation. *Sleep*, **27**, 1479–1485.

Sheroziya, M. & Timofeev, I. (2014) Global intracellular slow-wave dynamics of the thalamocortical system. *J. Neurosci.*, **34**, 8875–8893.

Steriade, M. (2006) Grouping of brain rhythms in corticothalamic systems. *Neuroscience*, **137**, 1087–1106.

Tamminen, J., Ralph, M.A.L. & Lewis, P.A. (2013) The role of sleep spindles and slow-wave activity in integrating new information in semantic memory. *J. Neurosci.*, **33**, 15376–15381.

Tewes, U. (1991) *HAWIE–R: Hamburg-Wechsler Intelligence Test for Adults: Handbook and Testing Instructions*. Huber, Stuttgart.

Tort, A.B.L., Komorowski, R., Eichenbaum, H. & Kopell, N. (2010) Measuring phase-amplitude coupling between neuronal oscillations of different frequencies. *J. Neurophysiol.*, **104**, 1195–1210.

Watson, D., Clark, L.A. & Tellegen, A. (1988) Development and validation of brief measures of positive and negative affect: the PANAS scales. *J. Pers. Soc. Psychol.*, **54**, 1063–1070.

Weigenand, A., Schellenberger Costa, M., Ngo, H.-V.V., Claussen, J.C. & Martinetz, T. (2014) Characterization of K-complexes and slow wave activity in a neural mass model. *PLoS Comput. Biol.*, **10**, e1003923.

Yu, Y.-Q., Xiong, Y., Chan, Y.-S. & He, J. (2004) *In vivo* intracellular responses of the medial geniculate neurones to acoustic stimuli in anaesthetized guinea pigs. *J. Physiol.*, **560**, 191–205.

Zar, J.H. (1999) *Biostatistical Analysis*, 4th Edn. *vol 1*. Prentice Hall, Upper Saddle River, NJ, pp. 389–394.